

## Ab initio studies of the effect of nanoclusters on magnetostriction of Fe<sub>1-x</sub>Ga<sub>x</sub> alloys

Hui Wang,<sup>1,2</sup> Y. N. Zhang,<sup>3</sup> Teng Yang,<sup>2</sup> Z. D. Zhang,<sup>2</sup> L. Z. Sun,<sup>1</sup> and R. Q. Wu<sup>3,a)</sup>

<sup>1</sup>Department of Civil and Environmental Engineering, University of California, Irvine, California 92697-2175, USA

<sup>2</sup>Shenyang National Laboratory of Materials Science, Institute of Metal Research and International Centre of Materials Physics, Chinese Academy of Sciences, Shenyang 110016, People's Republic of China

<sup>3</sup>Department of Physics and Astronomy, University of California, Irvine, California 92697-4575, USA

(Received 4 October 2010; accepted 7 December 2010; published online 30 December 2010)

Using the density functional calculations, we investigated the effect of nanoprecipitation on the magnetostriction of Fe<sub>1-x</sub>Ga<sub>x</sub> alloys. While the B2-like FeGa clusters undergo slight tetragonal distortion, D0<sub>3</sub>-like FeGa clusters remain cubic in the Fe matrix. Moreover, we found that B2-like nanostructures produce negative magnetostriction, whereas D0<sub>3</sub>-like nanostructures give small positive magnetostriction in the hypothetical inhomogeneous structures. Therefore, the formation of nanoscale precipitates cannot be the reason for the extraordinary enhancement of magnetostriction of Fe<sub>1-x</sub>Ga<sub>x</sub> alloys. © 2010 American Institute of Physics. [doi:10.1063/1.3533659]

It is a challenging and exciting task to find new materials that exhibit high magnetostriction in a relatively low magnetic field for technological innovations.<sup>1</sup> Terfenol-D (Tb<sub>x</sub>Dy<sub>1-x</sub>Fe<sub>2</sub>) alloys show a giant magnetostrictive strain of a few thousand ppm and are now widely used in devices such as microelectromechanical system (MEMS), energy-harvesters, transducers, and sensors.<sup>2,3</sup> Galfenol (Fe<sub>1-x</sub>Ga<sub>x</sub>) alloys appear to be promising magnetostrictive and multi-function materials for the next generation because of their low cost, excellent ductility, and low saturation field.<sup>4</sup> Clark *et al.*<sup>5-7</sup> demonstrated that Galfenol alloys with  $x=19\%$  may have a large tetragonal magnetostriction,  $\lambda_{001} \sim 400$  ppm at a saturation field of 100 Oe, about 20 times stronger than that of the bulk Fe. Further development of these alloys for practical utilizations requires comprehensive understanding of the mechanism that leads to such tremendous enhancement in magnetostriction.<sup>5</sup> Recent *ab initio* studies for Fe<sub>1-x</sub>Ga<sub>x</sub> ( $x < 19\%$ ) and related alloys satisfactorily reproduced experimental results, indicating that the intrinsic Ga-induced change in electronic structures plays an essential role.<sup>8,9</sup> In contrast, extrinsic mechanisms such as the field induced rotation of D0<sub>3</sub>-D0<sub>22</sub> precipitates have also been proposed as the origin of the dramatic enhancement of magnetostriction of Galfenol.<sup>10</sup> The validity of such extrinsic model relies on the structural instability of the bulk D0<sub>3</sub> Fe<sub>3</sub>Ga, which was indeed found and explained in our recent density functional calculations.<sup>11</sup> However, D0<sub>3</sub> nanoparticles are actually embedded in the matrix of A2-Fe/Ga mixture in real samples. It is hence crucial to investigate the structural stability and magnetostrictive responses of small D0<sub>3</sub> clusters under a constrained condition.

In this letter, we report results of density functional theory studies of B2-like and D0<sub>3</sub>-like nanostructures embedded in the Fe matrix to test the applicability of the extrinsic model. Strikingly, we found that the confined D0<sub>3</sub>-like clusters retain their cubic shape and show a very small positive magnetostriction. This defies the basis of the extrinsic model that uses the field-driven reorientation of distorted

nanoprecipitates as the cause of extraordinary magnetostriction of Galfenol. The B2-like nanostructures show sizable tetragonal distortion, in good accordance to experimental findings.

The *ab initio* electronic structure calculations and structural relaxations were performed with the Vienna *ab initio* simulation package (VASP).<sup>12</sup> The spin-polarized generalized gradient approximation was employed to describe the exchange and correlation interactions among electrons, using the Perdew–Burke–Ernzerhof functional.<sup>13</sup> We treated the Fe-3d4s4p and Ga-3d4s4p shells as valence states and adopted the projector-augmented wave method to represent the effect of the ionic cores.<sup>14</sup> The energy cutoff for plane-wave expansion was 400 eV, sufficient for Fe–Ga systems according to test calculations. For the 128-atom unit cell, a 4×4×4 Monkhorst–Pack *k*-point mesh in the Brillouin zone was used to evaluate integrals in the reciprocal space. For the determination of magnetic anisotropy energies and magnetostrictive coefficients, self-consistent calculations with the spin-orbit coupling term were performed in the non-collinear mode of the VASP, as implemented by Hobbs *et al.*<sup>15</sup> The criterion for structural optimization required the atomic force on each atom smaller than 0.01 eV/Å.

To begin with, the total energies of the bulk Fe<sub>3</sub>Ga in either B2-like or D0<sub>3</sub> phase are presented in Fig. 1, versus the tetragonal lattice distortion. For the B2-like structure, total energy decreases monotonically as the lattice expands along the *z*-axis, until the fcc-type L1<sub>2</sub> structure is formed. The D0<sub>3</sub> phase of Fe<sub>3</sub>Ga is also unstable against the tetragonal distortion and the optimized *c/a* ratio is 1.23. Accordingly, the tetragonal shear modulus of the D0<sub>3</sub>-Fe<sub>3</sub>Ga bulk is negative  $C=(C_{11}-C_{12})/2=-3.1$  GPa, with the theoretically optimized lattice size ( $a=5.75$  Å). Electronic structure analysis indicates that the instability of the cubic D0<sub>3</sub>-Fe<sub>3</sub>Ga is driven by the presence of an antibonding Fe-*e<sub>g</sub>* state at the Fermi level in the majority spin channel. Interestingly, as shown in the inset of Fig. 1, our calculations show that *C'* changes its sign when the lattice size slightly shrinks by as small as 0.2% to  $a=5.74$  Å. Therefore, it is unclear if D0<sub>3</sub>-Fe<sub>3</sub>Ga nanoparticles still undergo tetragonal distortion if

<sup>a)</sup>Electronic mail: wur@uci.edu.

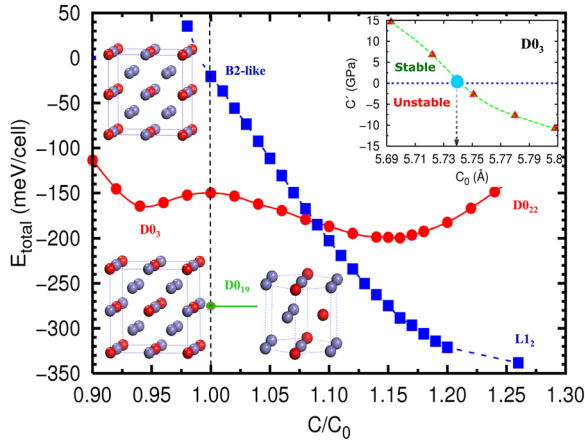


FIG. 1. (Color online) Strain dependent total energies of the bulk  $\text{Fe}_3\text{Ga}$  crystal in the B2-like (blue or dark gray square) and  $\text{D0}_3$  (red or gray circle) structures. The green dot indicates the energy of the hexagonal  $\text{D0}_{19}$  structure aside. The left insets give the B2-like and  $\text{D0}_3$  structures. The right inset shows values of  $C'$  for the bulk  $\text{D0}_3\text{-Fe}_3\text{Ga}$  with different lattice sizes.

they are embedded in Fe or A2 Fe/Ga matrices. This inspires us to directly investigate the structural and magnetic properties of several B2-like and  $\text{D0}_3$ -like nanoclusters in the matrix of bcc Fe, using models that contain 128 atoms, as shown in Fig. 2. No constraint was assumed for the shape and size of the unit cells, and all atoms were allowed to relax during the structural optimization procedure.

The lattice constants of the unit cell in Fig. 2(a) are  $a=b=11.353$  Å and  $c=11.395$  Å for the small B2-like nanostructure. The corresponding values for the large B2-like nanostructure depicted in Fig. 2(c) are  $a=b=11.374$  Å and  $c=11.643$  Å. Obviously, the entire unit cell expands under the influence of the B2-like FeGa clusters, but the clusters do not stretch to the  $\text{L1}_2$  structure as for the uniform B2-like bulk  $\text{Fe}_3\text{Ga}$ , as displayed in Fig. 1. As a validation of the present studies, the calculated distance between adjacent Ga atoms is 2.990 Å, a value that agrees excellently with the experimental data extracted from the differential x-ray absorption spectroscopy.<sup>16</sup> We found that the Fe columns near the Ga pairs also slightly expand along with their Ga neighbors. For example, the vertical Fe–Fe second neighbor distance near Ga becomes 2.846 Å, about 0.012 Å larger than the corresponding value in the bulk Fe. For the large B2-like nanocluster shown in Fig. 2(c), the Fe–Fe second neighbor distance becomes 2.926 Å near Ga. Clearly, B2-like clusters still tend to go through the bcc  $\rightarrow$  fct transition, but the distortion is largely limited by the bcc Fe matrix.

Importantly, the two  $\text{D0}_3$ -like nanostructures shown in Figs. 2(b) and 2(d) retain their cubic structures in the Fe matrix. The optimized lattice constants for the unit cells with small and large  $\text{D0}_3$ -like nanostructures are  $a=b=c$

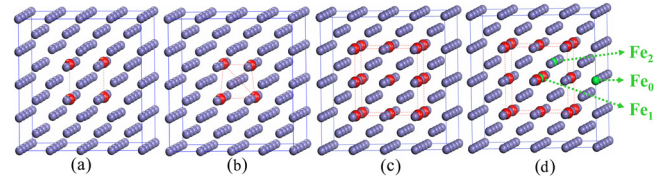


FIG. 2. (Color online) Schematic models for  $\text{Fe}_{1-x}\text{Ga}_x$  alloys with clusters in (a) small B2-like,  $x=3.125\%$ ; (b) small  $\text{D0}_3$ -like,  $x=3.125\%$ ; (c) large B2-like,  $x=11.7\%$ ; and (d) large  $\text{D0}_3$ -like,  $x=10.9\%$ . The purple (dark gray) and red (gray) balls are for Fe and Ga atoms, respectively.

$=11.367$  Å and  $a=b=c=11.450$  Å, respectively. The lack of tetragonal distortion of embedded  $\text{D0}_3$ -like  $\text{Fe}_3\text{Ga}$  clusters, at least in the subnanometer length scale, challenges the assumption of the extrinsic mechanism of giant magnetostriction of Fe–Ga alloys.<sup>11</sup> Recent experimental work also indicates that the formation of nanoclusters will not lead to substantial enhancement of magnetostriction in these alloys.<sup>17</sup> According to the binding energies in Fig. 1, the constrained ( $c/c_0=1$ ) uniform B2-like  $\text{Fe}_3\text{Ga}$  crystal is higher in energy than its  $\text{D0}_3$  counterpart. Similarly, the structure in Fig. 2(a) is also higher in energy than that in Fig. 2(b), by  $\sim 130$  meV/cell.

We further directly explore the intrinsic effect of Ga clustering on the magnetostriction of Galfenol. The supercells were deformed along the  $z$ -axis with a strain  $\varepsilon$ . We adopted the constant-volume mode ( $\varepsilon_x=\varepsilon_y=\varepsilon/2$ ), and the atomic positions were fully optimized for each tetragonal strain. The strain-dependent total energies and magnetocrystalline anisotropic energies were calculated, and the data are displayed in Fig. 3. The values of  $\lambda_{001}$  were determined through the formula<sup>18</sup>

$$\lambda_{001} = \frac{2dE_{\text{MCA}}/d\varepsilon}{3d^2E_{\text{total}}/d\varepsilon^2}. \quad (1)$$

To see if the VASP is reliable for the determination of magnetostriction, we first performed benchmark calculations for both uniform B2-like and  $\text{D0}_3$  bulk  $\text{Fe}_3\text{Ga}$  alloys; and found that the results of  $dE_{\text{MCA}}/d\varepsilon$  satisfactorily reproduce our previous data obtained through all-electron calculations.<sup>18</sup>

It is interesting that the magnetostrictive coefficients of both B2-like and  $\text{D0}_3$ -like cluster structures in Figs. 3(a) and 3(b) are opposite in sign compared to the results of their bulk counterparts.<sup>18</sup> For instance, the calculated  $\lambda_{001}$  for the large B2-like structure in Fig. 2(c) is  $-33$  ppm. This is in direct contrast to the perception that local B2 structure always leads to positive magnetostriction. On the other hand,  $\lambda_{001}$  for the embedded  $\text{D0}_3$  structure in Fig. 2(d) is positive,  $+45$  ppm. According to experiments and also our previous density functional calculations,<sup>9</sup>  $\lambda_{001}$  of Galfenol samples at Ga concentration about  $\sim 11\%–12\%$  should be around  $+120$  ppm,

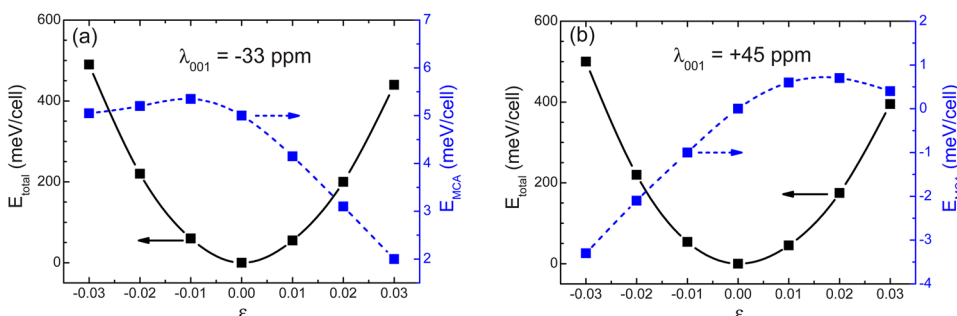


FIG. 3. (Color online) Strain dependent total energies (black lines) and magnetocrystalline anisotropy energies (blue or gray lines) of (a) the B2-like and (b) the  $\text{D0}_3$ -like Fe–Ga cluster in the unit cells, as depicted in Figs. 2(c) and 2(d), respectively.

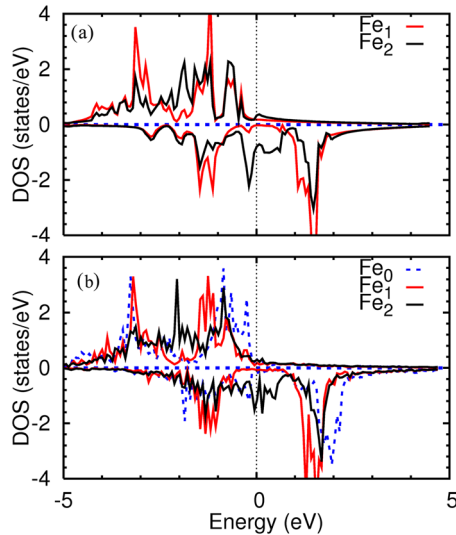


FIG. 4. (Color online) Partial density of states of selected Fe atoms in (a) the bulk  $D0_3$ - $Fe_3Ga$  and (b) the embedded  $D0_3$  FeGa cluster. Notations for Fe atoms follow those given in Fig. 2(d).

if the homogeneous A2 structure is assumed. This clearly indicates that the inhomogeneous precipitations are detrimental for the enhancement of magnetostriction, and they should be very unlikely to form in real samples at this Ga concentration.

As known, the enhancement of magnetostriction in Fe–Ga alloys stems from the presence of nonbonding states around the Fermi level, and the sign of magnetostriction or strain-induced magnetic anisotropy typically depends on the wave function features of several key occupied-unoccupied states. Detailed discussions in this aspect can be found in our previous publications for several related alloys.<sup>19</sup> To see why clustering alters magnetostriction so drastically, here we show the local density of states (DOS) of the large  $D0_3$ -like cluster in Fig. 4, along with the corresponding results of the bulk  $D0_3$ - $Fe_3Ga$ . The pronounced nonbonding peaks for the  $Fe_2$  atom, indicative of the broken Fe bonds toward Ga atoms, can be seen in both cases. However, there are several distinguishable differences between DOS curves in Figs. 4(a) and 4(b). (1) The majority spin  $d$ -bands of  $Fe_1$  and  $Fe_2$  are slightly lowered in energy in the cluster case, (2) the small  $e_g$ -peak at  $E_f$  of  $Fe_2$  in the majority spin channel disappears in the cluster case, and (3) the  $Fe_2$   $d$ -bands shift to the high energy side and have more fine structures around the Fermi level in the minority spin channel. In addition, DOS curves of the  $Fe_0$  atom also differ from that of the bulk Fe; a small amount of holes in the majority spin channel and a broad dip in the minority spin channel can be seen. Therefore, the electronic effect of Fe–Ga clustering extends to a large distance in the Fe matrix, to at least the third rank neighbors.

We want to point out that  $D0_{22}$  is not a stable structure either for the uniform bulk  $Fe_3Ga$ , according to the data in Fig. 1. Furthermore, the hexagonal  $D0_{19}$  and cubic  $L1_2$  phases are much lower in energy than the  $D0_3$ / $D0_{22}$  structures. Therefore, precipitations should be more likely to adopt  $D0_{19}$  and  $L1_2$  phases rather than the  $D0_{22}$  phase. The observation of elongated  $D0_3$ -like precipitates in Galfenol samples reported by Cao *et al.*<sup>20</sup> was questioned by more recent studies using x-ray diffuse scattering.<sup>21</sup> It was also found that  $Fe_{73.4}Ga_{25}Ge_{1.6}$  sample, with a small addition of Ge, has two phases: the fcc  $L1_2$  and the hexagonal  $D0_{19}$ , in

agreement with our analysis.<sup>22</sup> Therefore, we believe that the present density functional studies provide reliable energetics for the understanding of the structural and magnetic properties of Galfenol alloys.

In summary, our *ab initio* studies for the embedded  $Fe_{1-x}Ga_x$  clusters challenge the basic assumption of the extrinsic mechanism<sup>10</sup> for the strongly enhanced magnetostriction of Galfenol. While B2-like nanostructures deform slightly from their cubic shape,  $D0_3$ -like nanostructures show no tetragonal distortion when they are embedded in the Fe matrix. The intrinsic magnetostriction of FeGa clusters is also much smaller than the homogeneous A2 structure at the same Ga composition. Therefore, there should be no significant precipitation in Galfenol samples with Ga concentration of  $\sim 12\%$  or lower.

We are indebted to Dr. A. E. Clark, Dr. K. B. Hathaway, and Dr. M. Wun-Fogle at the NSWC, and Professor A. B. Flatau at the University of Maryland for simulative discussions. This work was supported by the ONR (Grant No. N00014-08-1-0143). H.W., L.Z.S., and Z.D.Z. also acknowledge the support from the CAS/SAFEA International Partnership Program for Creative Research Teams. Part of the calculations was conducted on DoD supercomputers, while the rest was performed on the supercomputers in the CAS Shenyang National Laboratory of Materials Sciences.

<sup>1</sup>H. Szymczak, *J. Magn. Magn. Mater.* **200**, 425 (1999).

<sup>2</sup>A. E. Clark, in *Ferromagnetic Materials*, edited by E. P. Wohlfarth (North-Holland, Amsterdam, 1980), Vol. 1, p. 531.

<sup>3</sup>A. V. Andreev, in *Handbook of Magnetic Materials*, edited by K. H. J. Bushow (Elsevier, Amsterdam, 1995), Vol. 8, p. 59.

<sup>4</sup>E. M. Summers, T. A. Lograsso, and M. Wun-Fogle, *J. Mater. Sci.* **42**, 9582 (2007).

<sup>5</sup>A. E. Clark, J. B. Restorff, M. Wun-Fogle, T. A. Lograsso, and D. L. Schlageel, *IEEE Trans. Magn.* **36**, 3238 (2000).

<sup>6</sup>J. R. Cullen, A. E. Clark, M. Wun-Fogle, J. B. Restorff, and T. A. Lograsso, *J. Magn. Magn. Mater.* **226–230**, 948 (2001).

<sup>7</sup>A. E. Clark, K. B. Hathaway, M. Wun-Fogle, J. B. Restorff, T. A. Lograsso, V. M. Keppens, and G. Petculescu, *J. Appl. Phys.* **93**, 8621 (2003).

<sup>8</sup>J. X. Cao, Y. N. Zhang, W. J. Ouyang, and R. Q. Wu, *Phys. Rev. B* **80**, 104414 (2009).

<sup>9</sup>Y. N. Zhang, J. X. Cao, and R. Q. Wu, *Appl. Phys. Lett.* **96**, 062508 (2010).

<sup>10</sup>A. G. Khachatryan and D. Viehland, *Metall. Mater. Trans. A* **38**, 2317 (2007); S. Bhattacharyya, J. R. Jinschek, A. G. Khachatryan, H. Cao, J. F. Li, and D. Viehland, *Phys. Rev. B* **77**, 104107 (2008).

<sup>11</sup>Y. N. Zhang and R. Q. Wu (unpublished).

<sup>12</sup>G. Kresse and J. Hafner, *Phys. Rev. B* **49**, 14251 (1994).

<sup>13</sup>J. P. Perdew, K. Burke, and M. Ernzerhof, *Phys. Rev. Lett.* **77**, 3865 (1996).

<sup>14</sup>G. Kresse and D. Joubert, *Phys. Rev. B* **59**, 1758 (1999).

<sup>15</sup>D. Hobbs, G. Kresse, and J. Hafner, *Phys. Rev. B* **62**, 11556 (2000); M. Marsman and J. Hafner, *ibid.* **66**, 224409 (2002).

<sup>16</sup>M. P. Ruffoni, S. Pascarelli, R. Grössinger, R. Sato Turtelli, C. Bormion-Nunes, and R. F. Pettifer, *Phys. Rev. Lett.* **101**, 147202 (2008).

<sup>17</sup>C. Mudivarthi, Ph.D. thesis, University of Maryland, 2010.

<sup>18</sup>R. Q. Wu, *J. Appl. Phys.* **91**, 7358 (2002).

<sup>19</sup>Y. N. Zhang, J. X. Cao, I. Barsukov, J. Lindner, B. Krumm, H. Wende, and R. Q. Wu, *Phys. Rev. B* **81**, 144418 (2010).

<sup>20</sup>H. Cao, P. M. Gehring, C. P. Devreugd, J. A. Rodriguez-Rivera, J. Li, and D. Viehland, *Phys. Rev. Lett.* **102**, 127201 (2009).

<sup>21</sup>Y. Du, M. Huang, S. Chang, D. L. Schlageel, T. A. Lograsso, and R. J. McQueeney, *Phys. Rev. B* **81**, 054432 (2010).

<sup>22</sup>G. Petculescu, K. L. Ledet, M. Huang, T. A. Lograsso, Y. N. Zhang, R. Q. Wu, M. Wun-Fogle, J. B. Restorff, A. E. Clark, and K. B. Hathaway, “Magnetostriction, elasticity, and  $D0_3$  phase stability in Fe-Ga-Ge alloys”, *J. Appl. Phys.* (to be published).